Surface Modification for High-Reliability and Multi-Functional Hybrid Interconnections

Akitsu Shigetou

Principal Researcher, Team Leader,
Smart Interface Team,
Research Center for Materials Nanoarchitectonics (MANA),
National Institute for Materials Science (NIMS)
Concurrently: Visiting Professor, the University of Tokyo

Guest Seminar @ State University of New York at Binghamton
2025/04/30

0

Outline

Points of my talk:
- Importance on surface/interface design to create functions
- **Bonding & debonding in single process**

1. Research backgrounds :
   1.1. Interfaces for Cutting-Edge Applications
   1.2. Essential Surface/Interface Characteristics
2. Lineage to **Low-Temp, Non-Vacuum, Reliable Hybrid Bonding**
   2.1. Direct Bonding Using High Vac (1990s)
   2.2. Half Non-Vac Process (early 2000s)
   2.3. **VUV-Based** Non-Vac Process (around 2007~)
   2.4. New VUV-Based Process (around 2010~)
3. For "Cradle to Grave" Tech: **Bondability and Debondability**
   3.1. Trigger of "**Solid-State Debonding**"
   3.2. Process Design
   3.3. Bondability & Debondability
4. Summary

Before Getting Started

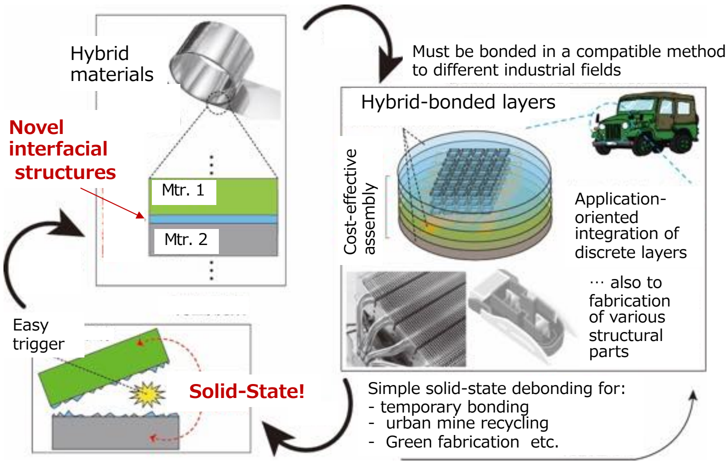

0. What we are

Team for surface and interface design to create multiple functions

- A. Shigetou (Team leader)
- Two post-doctoral researchers from India and China
- Two Ph. D. candidates from Taiwan
- 3 technicians

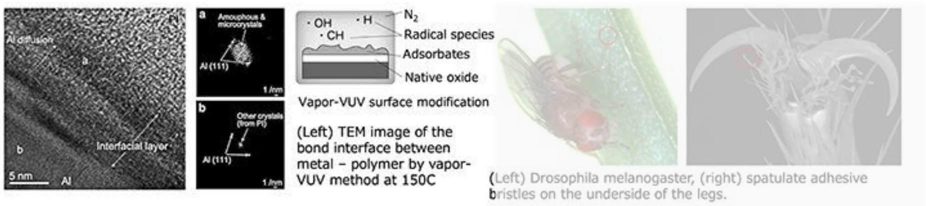

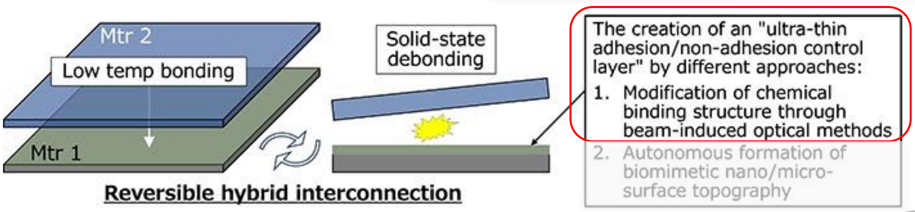

Features of NIMS Internship Program

NIMS is Japan's sole national research institute specialized in materials science. We have created a number of materials that made a global impact. Our mission is to pave the way for a better future for humankind by solving issues in environment, energy, medicine, and infrastructure, focusing on advanced research and development of innovative materials including metals, ceramics, polymers and optical materials.

We promote the shared use of our world's leading research equipment and facilities with other institutes and accept a number of researchers and students from all over the world to train researchers and engineers who can be internationally competitive. As part of it, we provide NIMS Internship program and accept students enrolled in university and graduate school as intern. The participants can take part in the leading edge research studies at NIMS. For the outstanding students we provide financial support.

If you would like to use the world's leading research equipment and facilities, take part in the cutting-edge research projects and meaningful interactions with researchers from all over the world. We are looking forward to your application.

Benefits

- Experience cutting-edge research activities ▶ Develop skills for your career planning
- Participate in some of our exclusive seminars at NIMS ▶ Enhance your presentation skills
- Interaction with highly-motivated students ▶ Get connected to an interdisciplinary professional network

2

4

International Cooperative Graduate Program

Co-supervision of doctoral students with overseas partner universities

As of August 1st, 2022

Asia	15
Europe	10
North America	4
Oceania	1
Total	30

- NIMS supports living expenses of graduate students in Tsukuba for up to 12 months in the course of their Ph.D. study
- Partner universities support travel expenses of their students

5

5

1. Research Backgrounds

1.1. Interfaces for Cutting-Edge Applications

The better tunability of interfaces the better system performances

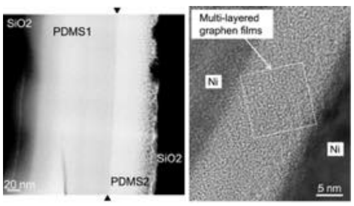

Semi direct-bonded interfaces of (Left) PDMS and (Right) multi-layered graphene: Shigetou et al., IEEE NANO 2012 etc.

Transparency, conductivity, carrier/electron mobility...

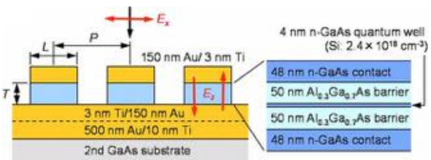

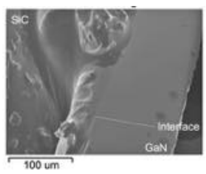

(Up) Quantum well IR photodetectors and (down) semi direct-bonded GaN / SiC interface: Shigetou et al., ECTC 2015 and Miyazaki et al., 4th A3 MetaMtr. Forum 2019, respectively.

Adhesion, responsivity, bandgap, diffusivity, reliability...

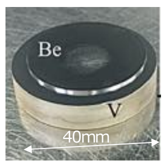

Direct-bonded Be-V for neutron excitation target

Atomic scale → Nano/micro scale → Large scale

Crystallinity

Chemical binding structure and layer thickness

Bond mechanism

Contact mechanics

Fracture mechanics

1.1. Interfaces for Cutting-Edge Applications

Automotive IoT: Seamless signal transmission via structural materials

- "Systems in Materials" packaging
- Integration regardless of materials and fabrication scales
- Seamless bonding: Use of **intrinsic surface properties**

Electronics Packaging: nm – um, deep knowledge on surfaces/interfaces, special fabrication atmosphere acceptable

→ **Industrially simple hybrid bonding scheme**

Fabrication scale [m]

10^{-9} 10^{-8} 10^{-7} 10^{-6} 10^{-5} 10^{-4} 10^{-3} 10^{-2} 10^{-1} 10^{0} 10^{1}

Carbon/glass fibers Bio-mimetic matr | Electronics for SMART automotives (Biosensors, RF, anti-shock & heat etc.) | SMART & robust structural matr Power / green electronics etc.

1.2. Essential Surface/Interface Characteristics

- **Non-vacuum & low-temp** (around <150℃) for diverse materials ← Done
- High-reliability such as **anti-hydrolytic interface** ← Almost done
- **Easy solid-state debonding** ← Not yet

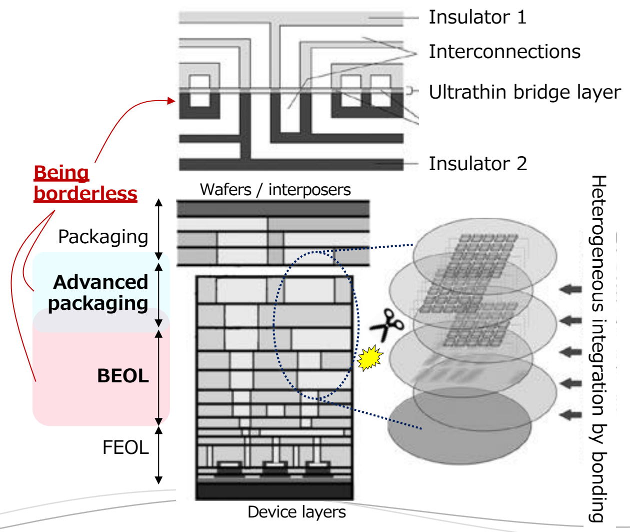

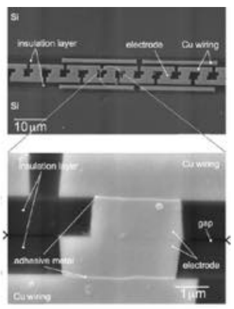

- Shigetou et al., Proc. 51st ECTC (2001)
- Shigetou et al., Trans. Adv. Pckg. (2007) etc.

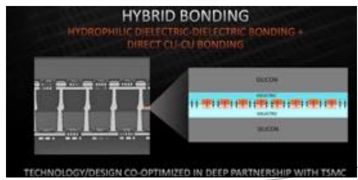

AMD Hotchips 2021 Sr. Fellow R. Swaminathan

1.2. Essential Surface/Interface Characteristics

NIMS

Hybrid interface must be seamless to:
- **Fabrication scale**
- **Material properties**

➕ Green technology (eco-logy)
Simple & low-cost (eco-nomy)

Thermoplasticity		Thermoset/Infusible	Metals
Crystalline	Noncrystalline		
PEEK	PEI	Polyimide (PI)	Hastelloy
PAEK	PPSU	Cyanate ester	Inconel/Stellite
PPS	PES	Bismaleimide	Ti, Ti alloys
LCP	PSU	Epoxy group	Al, Al alloys
PA	PC	Phenol group	Fe, Fe alloys
PBT	ABS	Unsaturated polyester	Stainless group
POM			Co, Cr, Cu
PP(S)			Noble metals

Example of structural materials officially used in automotive companies. Those in red letters are also utilized in electronic substrates and packaging.

- **Covalent/coordinate bond** regardless of the combination
- Chemically stable organic materials: Highly marketable in molding process

NIMS

2. Lineage to **Low-Temp, Non-Vacuum, Reliable** Hybrid Bonding

2.1. Direct Bonding Using High Vac (1990s)

Surface Activated Bonding (SAB) at RT : Use of dangling bonds

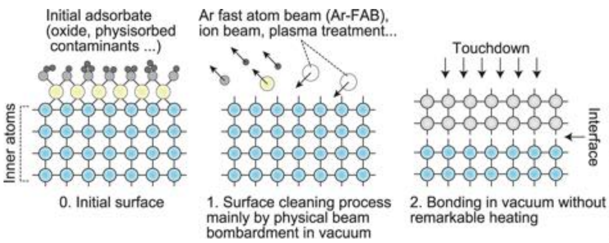

Bonding by attractive force btwn atomically clean surfaces :
- **Covalent/metal bond only**

Metals (metallic-bond): Au, Cu, Al, Sn, alloy ... Semiconductors (covalent-bond): Si, III-V ...
High density, direct interconnection ...
Vacuum condition (partially ambient air)
Room temperature or considerably low temp.

Change in chemical/physical surface conditions induced by beam irradiation

1) Minimum surface activation condition
2) Acceptable increase in surface roughness to ensure full contact
   1) + 2) = "clean & flat" surface
3) Acceptable adsorption from the environment to maintain bondability
   3) = Q-time

12

12

2.1. Direct Bonding Using High Vac (1990s)

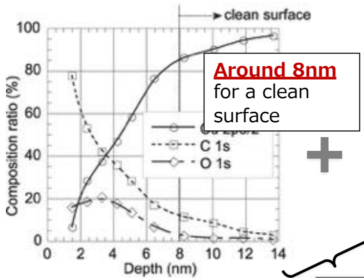

ビーム衝撃によるエッチング深さとCMP-Cu表面の化学的組成変化の関係

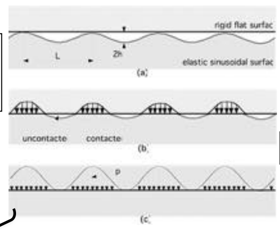

$$\frac{h^2}{L} < \frac{\Delta\gamma}{E^*} \cdot \frac{32(1-\nu_*^2)}{\pi} \quad \frac{1}{E^*} = \frac{1-\nu_1^2}{E_1} + \frac{1-\nu_2^2}{E_2}$$

or $E^* \sigma^{*\,3/2} \sqrt{\frac{K}{\pi}} \leq \gamma^*$

For CMP-Cu film : Ra **2nm**

Concept of Hertz's contact theory

Optimum process window for this CMP-Cu film:

Etching depth of 8 – 15 nm + vacuum exposure of less than 0.2 Pa*s.

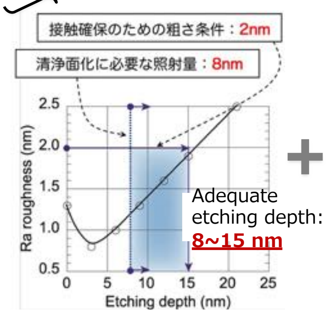

Change in mean surface roughness correspondence to the etching depth.

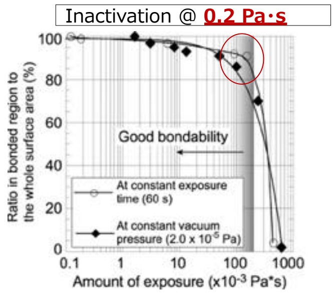

Relationship btwn the bonded area and the exposure amount to oxygen

13

13

2.1. Direct Bonding Using High Vac (1990s)

NIMS

World's first Cu-Cu bonding at RT

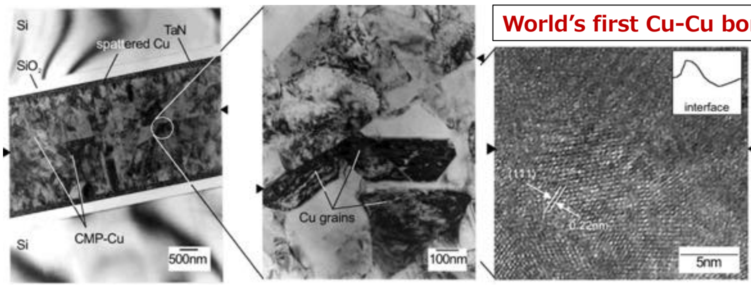

A. Shigetou et al., J. Surface Sci. 2001 など

SiO2 cannot be bonded by SAB method･･･？

Fe contamination from ion gun barrel worked as adhesive layer!

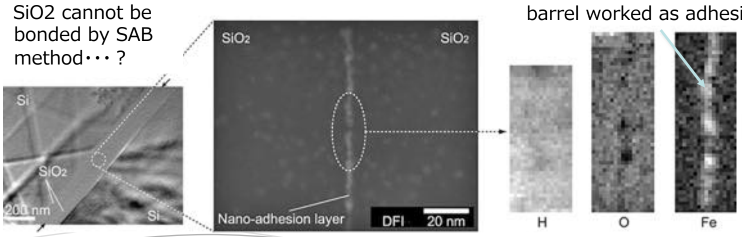

Idea of ultrathin bridge layer

2.2. Half Non-Vac Process (early 2000s)

NIMS

Cu-Cu Modified diffusion bonding supported by SAB : Cu-Cu bonding @ 150C via controlled thickness of native oxide

- High vac needs high cost → Working temp going high → All RT process really needed? → 100℃ higher than RT = 2 degrees up in diffusion coefficient!
- Tuning of surface inert layer (ex. native oxide) is necessary: **Thinner than volume diffusion distance of Cu ions!**

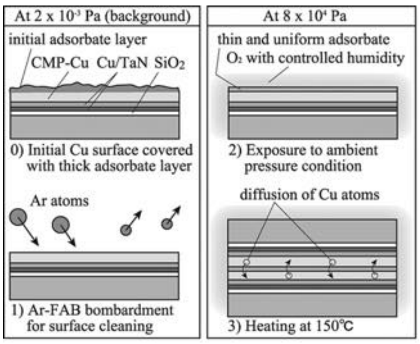

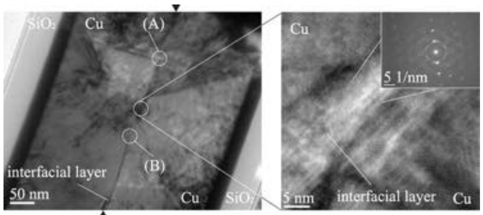

Shigetou et al., Appl. Phys. Exp. 2009.

Adhesive layer in non-vac atmosphere = **Tunable design of bridge structure**

2.3. VUV-Based Non-Vac Process (around 2007~)

NIMS

1. **Non-vac atmosphere** = Adhesion layer on the surface
2. Process tep lower than Tg = Less deformation & reaction
3. Less matrix damage

Use of light

Key of surface modification is on inorganic side

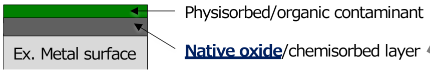

Covalent or ionic bond: High binding energy that cannot be dissociated with UV light only

Functional group	Binding energy		Wavelength (nm)
	kcal/mol	kJ/mol	
C≡C	188.8	791.1	151
C≡N	222.2	931.0	129
C=O	190.0	796.1	151
C=C	140.5	588.7	204
H−F	134.9	565.2	212
O=O	117.5	492.3	243
C−F	115.2	482.7	248
O−H	109.3	458.0	262
H−Cl	101.9	427.0	281
C−H	97.6	408.9	293
N−H	91.9	385.1	311
C−C	84.3	353.2	339
C−Cl	76.9	322.2	372
C−O	76.4	320.1	374
C−N	63.6	266.5	450

Developing bridging function in the adsorbed molecular layer in non-vac atmosphere

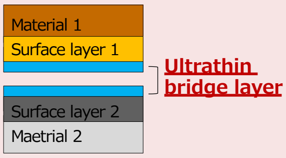

- Tunable chemical structure
- Tunable thickness
- Materials compatibility
- High bond strength
- High interfacial reliability

2.3. VUV-Based Non-Vac Process (around 2007~)

NIMS

Water vapor as the source of bridge layer

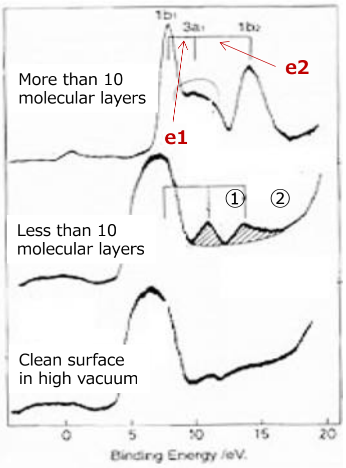

Change in valence band spectra of SrTiO3 concomitantly with increasing water adsorption
M. A. Henderson, Surf. Sci. Rep. 46 (2002)

Predictable adsorption behavior

① Lone pair of oxygen to cation sites
② Proton conduction on anion sites

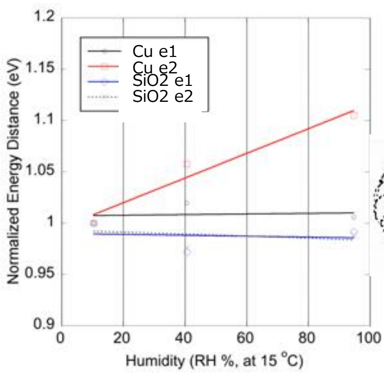

Change in the ground state of Cu and SiO2 at different humidity conditions

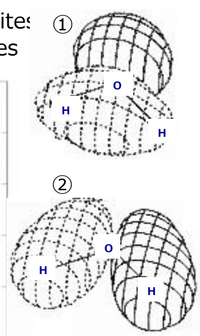

2.3. VUV-Based Non-Vac Process (around 2007~)

NIMS

Water Vapor-assisted ultraviolet (V-VUV) method : Highly modified hydrophilic bonding

- **In N2 atmosphere, <150℃**
- Bridge thickness ~10nm
- **“Exposure (s·kg/m³)”** as the process parameter
- Contact @ RT → Heating @150℃
- No bonding pressure is required in theoretically
- **Different interfacial functions by different solvents**

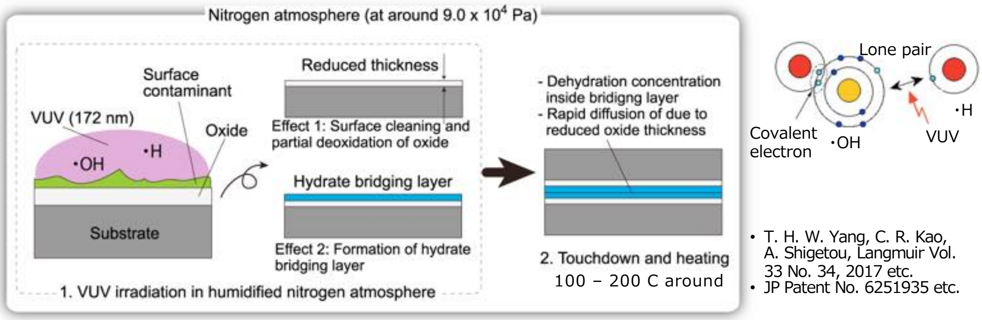

- T. H. W. Yang, C. R. Kao, A. Shigetou, Langmuir Vol. 33 No. 34, 2017 etc.
- JP Patent No. 6251935 etc.

Outline of V-VUV method in case of **WATER** vapor

18

2.3. VUV-Based Non-Vac Process (around 2007~)

NIMS

科学技術・大学 日刊工業新聞

Electronic Packaging

物材機構、異なる材料を水で接合する技術開発

2012/10/25 05:00

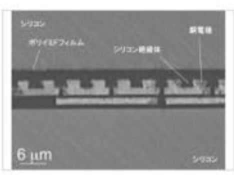

Newspaper article: The Daily Industrial (2012/10/25)

Cu-Cu Bumpless Interconnect for Hybrid Bonding. Cu-Cu, Cu-SiO₂, Cu-PI interfaces on the same plane @ 150 C.

Bio/Medica/Optical materials

PDMS – PDMS interface with transparency loss < 2%

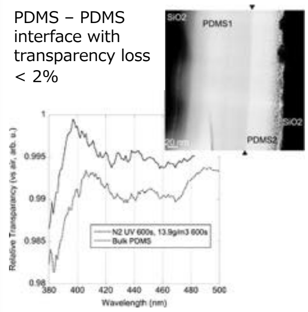

Structural Materials

CFRP – Steel, and PEEK - Ti64 bonding @ 150 – 200 C, including less thermal strain at the interfaces.

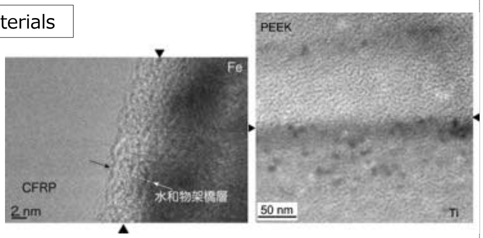

PEEK – Pt bonding for artificial bone parts

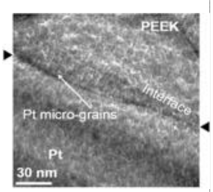

J. Elctr. Mtr. (2012), IEEE NANO (2012), Microelctr. Rel. (2016), Mtr. Sci. Eng. C. (2017) etc.

19

2.4 New VUV-Based Process (around 2010~)

NIMS

New tasks for water V-VUV method:

- **Hydrolysis degradation** : In particular @ inorganic – organic interfaces
- Different lifetime for different materials (will talk later)

- Target materials: **Cu, Al, Ti (Ti-6Al-4V), PEEK, PI, Si, SiC(N), GaN etc.**
- Water adsorption is hard to be avoided in actual IoT modules

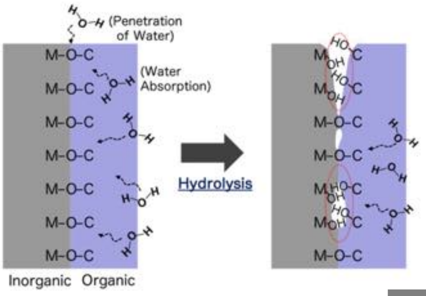

Irreviersible hydrolysis reaction at V-VUV interfaces :

Irreversible M-O-C (single oxygen bridge) hydrolysis at V-VUV bonding interfaces:

- Water penetration to interface
- Broken M-O- quickly forms chemically stable oxide
- Crack initiation due to stress concentration on unbonded oxide sites

So, let's make the hydrolysis reaction **equiriblium!**

20

2.4. New VUV-Based Process (around 2010~)

NIMS

Alkyl chains with hydroxyls at the and and **muti-dentate carboxylates** at the bottom (inorganic side)

Examples of Carboxylate (except for hydrogen bond)

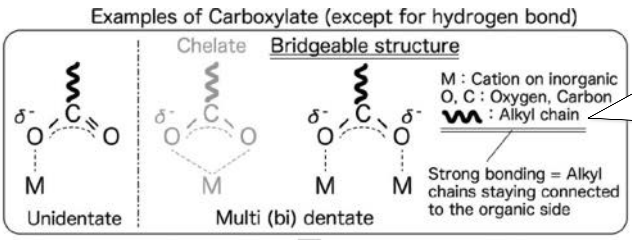

- Hydrophobicity can be tuned via alkyl chain length
- **Alkyl chain keeps connected to the other material**

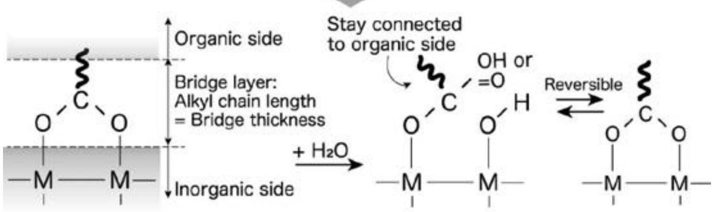

"One side is re-bonded while another one is disconnected"

Schematics of anti-hydrolysis bridge layer

21

2.4. New VUV-Based Process (around 2010~)

※ Example of Al – polyimide bonding

Alcohol - assisted VUV **(E or IPA-VUV) method** : As low-toxic source of **CH radical**

- **Use of atomized ethanol, IPA, etc.**
- Same process as water V-VUV: Exposure (**s·kg/m³**) as process parameter
- Batch process to water cleaning available in near future

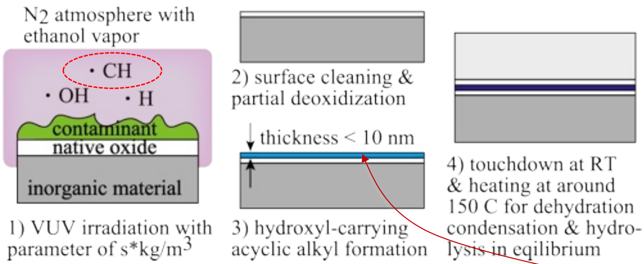

Outline of **Ethanol-VUV** surface modification / bonding method.

- Nature Scientific Reports 9 (2019)
- Materials & Design 195 (2020)
- JPN Patent No. 7018223
- CHN Patent No. IIC202391
- JPN Patent Application No. 2022-90266

etc.

- Pseud hydrophobic surface
- **Q-time longer than 24hrs for Si-relating materials**

2.4. New VUV-Based Process (around 2010~)

Major experimental procedures:

1. Ultrasonic washing: Acetone (only for Al) → ethanol → ultrapure water 1min each
2. VUV irradiation at different amounts of exposure **(s·kg/m³)**
3. X-ray photoelectron microscopy **(XPS)** for **overall check** of surface chemical binding status: 2x10⁻⁷Pa, Mg-Kα, 450W, detection at 15°, φ0.8mm
4. Fourier-transform IR spectroscopy **(FT-IR)** for **precise analysis on carbon** binding condition: After E-VUV, transferred to FT-IR equipment in air
5. Bonding: contact @RT, 0.04MPa, heating @ **150℃** for 10min
6. Transmission electron microscopy **(TEM)** & electron energy loss spctr. (EELS)

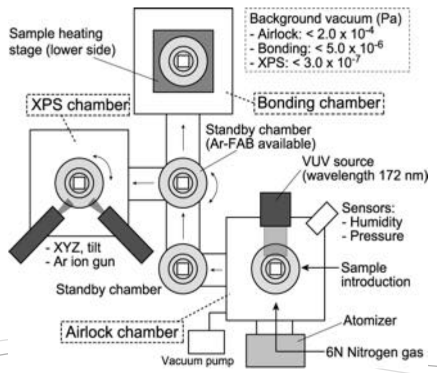

EB depo Al thin film on Si
(10 mm × 10 mm × 140 nm)

Si wafer

Polyimide (Kapton) thin film

Cut into

Polyimide (PI)
(15 mm × 15 mm × 25 um)

(LEFT) Schematic representation of E-VUV bonding apparatus including XPS/AES. E-VUV chamber equips ultrasonic atomizer and humidity/pressure sensors. (RIGHT) Outline of test vehicles.

2.4. New VUV-Based Process (around 2010~)

NIMS

Less matrix damage: ~2nm deep area is reorganized by V-VUV

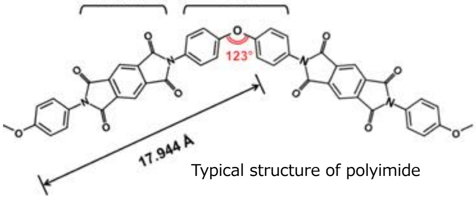

Typical structure of polyimide

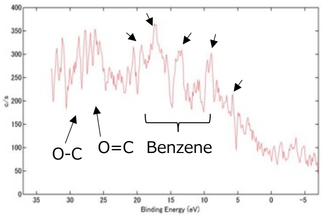

XPS valence spectrum of polyimide before beam irradiation

Both has "bondability"

Conventional beam process in high vac

VUV irradiation

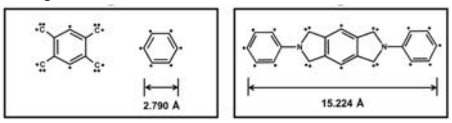

- fragmentation : C-O-C, C=O, C-N
- C concentration derives damages on dielectricity
- Low damage on matorix

Before irradiation
Ar-FAB bombardment in high vac

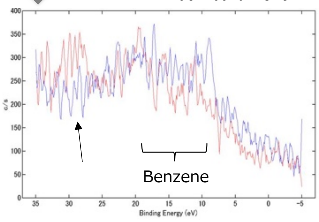

Yang, Kao, Shigetou, Langmuir 2017

24

2.4. New VUV-Based Process (around 2010~)

NIMS

Spectroscopy such as XPS is effective to identify the chemical species and atomic concentration, but not suitable to identify the chemical structure

- Al O1s specgra : -OH, C-OOH groups

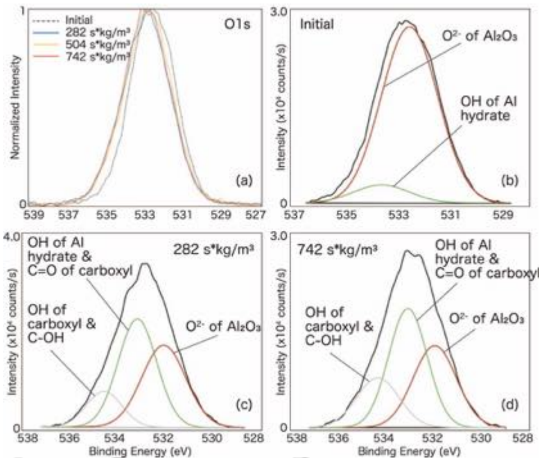

Al O1s spectra before/after E-VUV treatment. Black line indicates before irradiation, colored lines are for different exposure conditions.

(a) Spectra normalized with the highest intensity to highlight the difference in chemical binding conditions. FWHN increment due to –OH creation is seen.

(b)-(d) Results of curve fitting of spectra after E-VUV treatments. -OH and C-OOH peaks became apparent.

The layer thickness x can be calculated using the peak area obtained by the angle-resolved observations :

$$I_m = I_u \cdot e^{-x/\lambda_m \sin\Delta\theta}$$

I_m : Peak intensity of the targeted chemical component obtained at the detection angle θ_1
I_u : Peak area obtained at different angle
λ_m : Inelastic mean free path of the targeted bridge layer material

25

2.4. New VUV-Based Process (around 2010~)

NIMS

Bidentate Al carboxylate formation

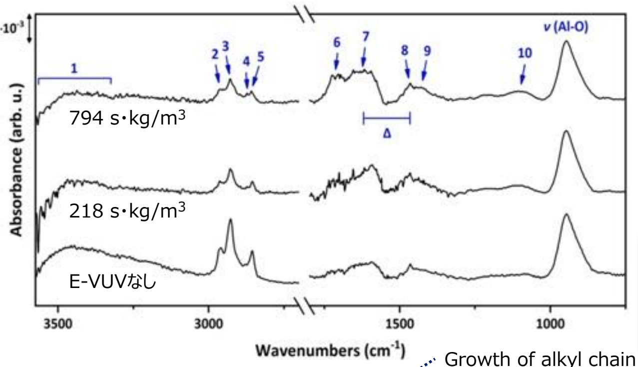

ATR-FTIR results showing the change in binding structure of C on Al surface after E-VUV treatment at different exposure conditions. Peaks at 1500 – 1700 cm^{-1} represents the formation of carboxylate.

$\Delta = \nu_{as} - \delta = 151\ cm^{-1}$

→ Bidentate

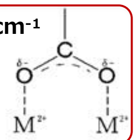

C. Ohe, J. Phys. Chem. B 103, 1999.

Growth of alkyl chain

No.	Wavelength (cm^{-1})	Assignment	No.	Wavelength (cm^{-1})	Assignment
1	3338–3504	ν(OH)	6	1703	ν(C=O) of COOH
2	2954	$\nu_{as}(CH_3)$	7	1616	$\nu_{as}(COO^-)$
3	2929	$\nu_{as}(CH_2)$	8	1465	$\delta(CH_2)$
4	2870	$\nu_s(CH_3)$	9	1430	$\nu_s(COO^-)$
5	2856	$\nu_s(CH_2)$	10	1108	ν(C–C–O) of $-CO_2R$ ester

26

2.4. New VUV-Based Process (around 2010~)

NIMS

Al (on native oxide)

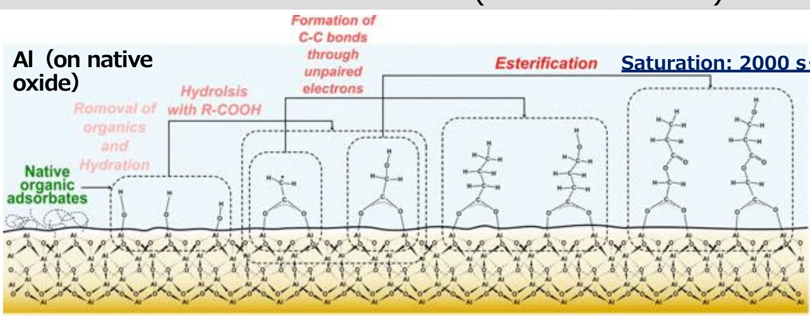

Polyimide

VUV-dissolved sites are occupied

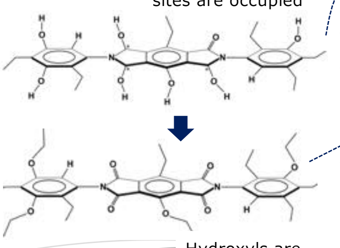

Hydroxyls are oxidized

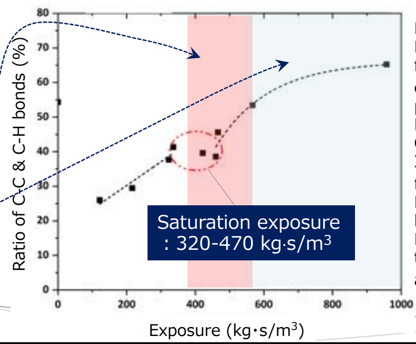

Ratio of C-C to C-H, meaning alkyl formation ratio, on PI surface with parameter of Exposure. Calculated from XPS C1s curve-fitted spectra. Layer growth linearly follows Exposure until all the reaction sites are occupied.

27

2.4. New VUV-Based Process (around 2010~)

No crack after storage testing at 85%RH·85℃ for more than 3 months

- As-bonded sample: Close adhesion via 10-nm-thick bridge layer
- After storage testing: **precipitation layer from Al side** for 20nm width

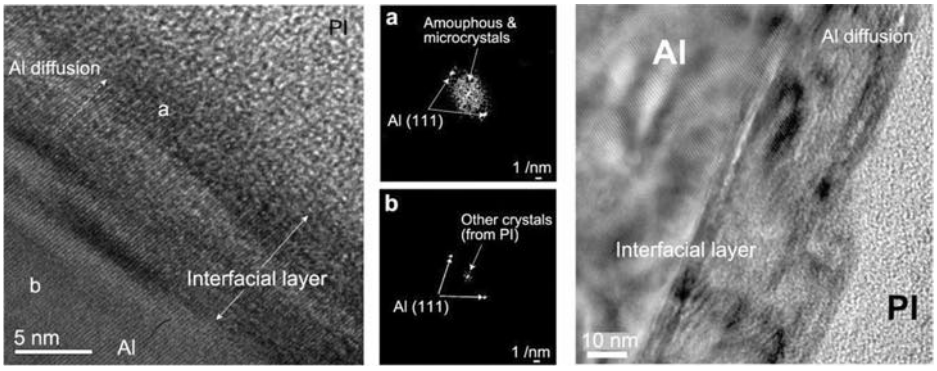

TEM images of the bond interfaces btwn Al and PI. Exposure amount of ethanol-VUV was **Al 1890 s·kg/m^3, PI 400 s·kg/m^3**. (Left) As-bonded interface, (Middle) diffraction spots at Point a & b, showing that the bridge layer is amorphous. (右) interface after 3 months of storage testing.

3. For "Cradle to Grave" Tech: Bondability and Debondability

※ Contents from JIEP/IEEE EPS/CPMT ICEP 2024 & 2025

※ From here Cu-Cu interface

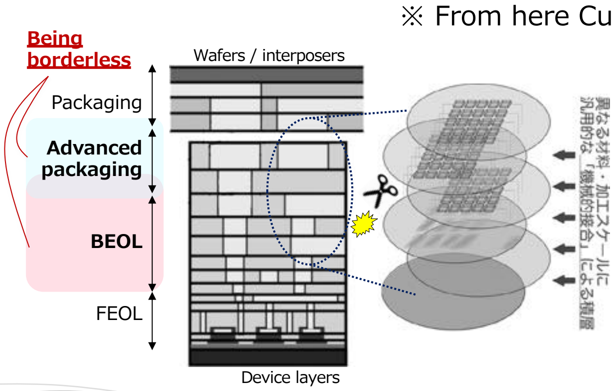

3.1. Trigger of "Solid-State Debonding"

- **Automatic nucleation** of oxide nanocrystals of inorganic materials
- Limited thickness growth of bridge layer

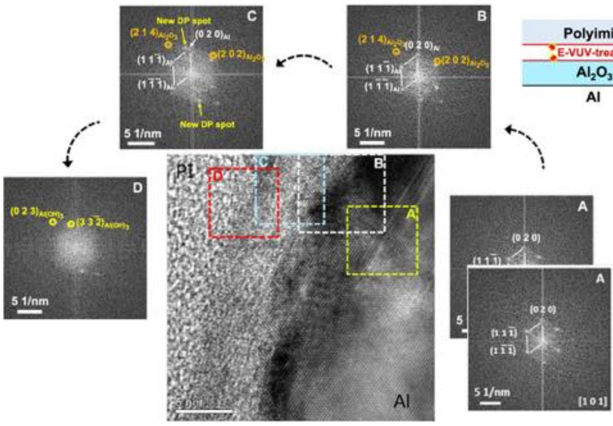

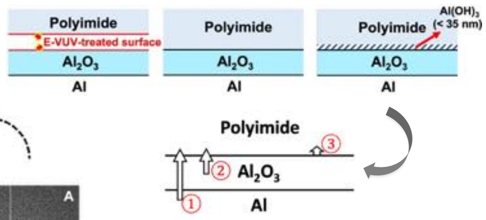

Possible source of $Al(OH)_3$:
③ The excess of Al ions produced by the reduction of the top surface of the natural oxide film by protons reacts with water molecules generated by dehydration condensation of bridge layer ends

TEM image of Al – polyimide interface bonded by the ethanol-VUV process. The interface was kept in 85℃・85%RH condition for more than 3 months.

T. Yang et a., Trans. JIEP 2019

3.1. Trigger of "Solid-State Debonding"

Bonding technology that incorporates debondindability

A clear "**trigge**r" for solid-state debonding at **low temperature** that does not overlap with actual operating or reliability test conditions.

- Trigger condition must be reached with existing industrial equipment.

Trigger: Set to about -100°C (can be reached in a common industrial freezer)

Concept of temperature-based solid-state debonding trigger. Sharp expansion only at the trigger temperature, showing the same thermal properties as common materials in an operation environment.

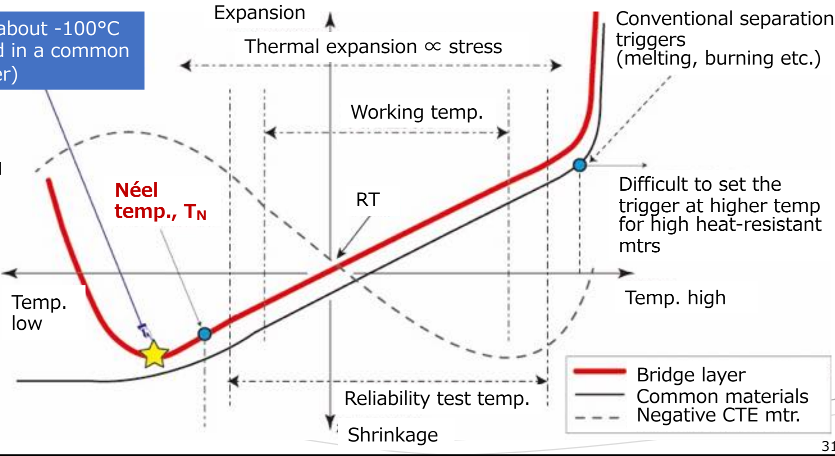

3.1. Trigger of ”Solid-State Debonding”

NIMS

Use of antiferromagnetic nanocrystals:

- Steep expansion at about -100°C: Due to **spin-lattice interaction** below Néel temp
- Especially for **CuO**: Volume strain of around **0.003** in Δ 20 C across the trigger

Use of the low-temperature expansion properties of some antiferromagnetic **nanocrystals**

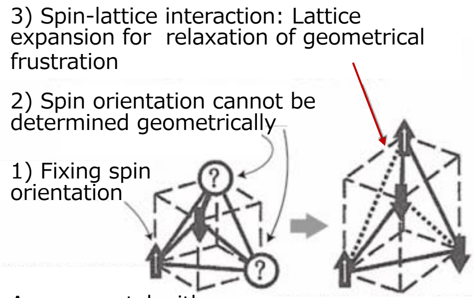

A nanocrystal with triangular spin configurations

Taken from: Kitani et al., Thermal Measurement 44 (2017)

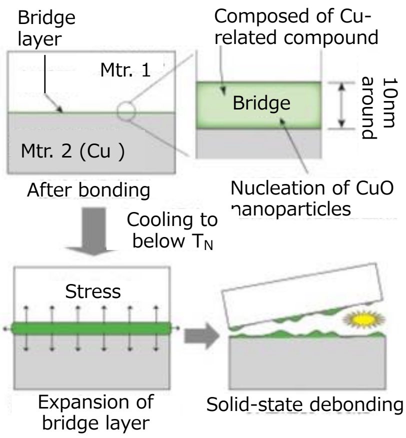

銅－銅積層体の分離方法及び銅－銅積層体，特許番号：07597418 登録日：2024-12-02
PCT/JP2022/027099 (EP, CN) , JP2021-115527

3.2. Process Design

NIMS

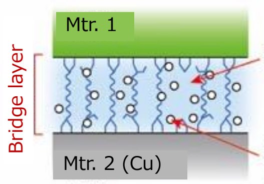

Concept of IPA-VUV bridge layer

Anti-hydrolytic bridge layer:
1) Dehydration condensation at the end of the bridge
2) Dynamic competition of hydrolysis

CuO nanocrystals:
Steep expansion at the temperature below T_N (around -100 C)

Test coupon : **Oxyten-free Cu plate**

- To investigate the evolution of chemical binding status only on Cu
- Highest purity (>99.96%) of Cu commercially available
- Used in various applications: lead frames, heat sinks, plating source, etc.

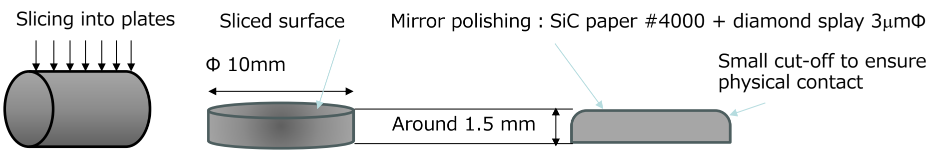

Schematic representation of Cu test coupon: Mean roughness (Ra) 10nm around

3.2. Process Design

NIMS

Chemical structure indicating bridge formation on Cu

1) hydroxide (due to ·OH) : Cu **– O – H** ← Checked with Cu2p3 spectra

2) Cu carboxylate at the bottom : **Cu – O –** R – C – OH (with =OH below the C)

Checked with Cu2p3 spectra

Checked with C1s spectra

Since the presence of native oxide is largest, the energy gaps from the native oxide peak were used to the curve fitting.

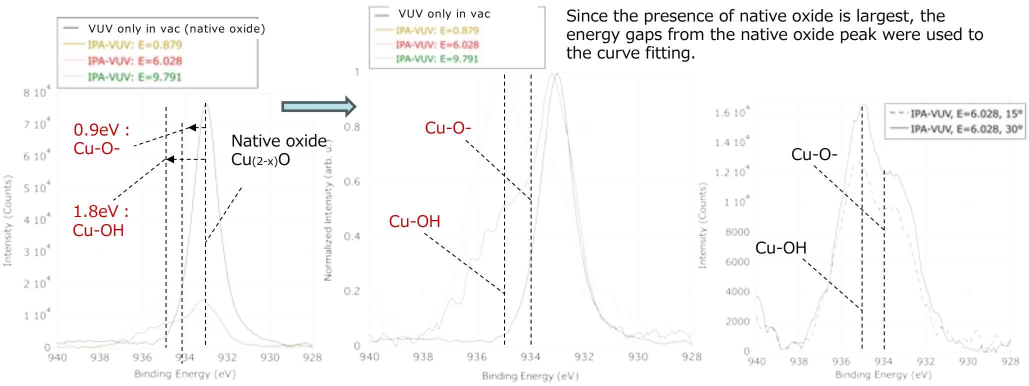

Cu2p3 spectra taken at 30° in different Exposure conditions

Normalized intensity to the maximum intensity in order to highlight the difference in binding conditions

Example of angle-resolved spectra at E=6.028. Taken at 15 and 30°.

34

3.2. Process Design

NIMS

Chemical structure indicating bridge formation on Cu

1) hydroxide (due to ·OH) : Cu – O – H

Checked with Cu2p3 spectra

2) Cu carboxylate at the bottom : Cu – O – R **– C – OH** (with **=OH** below the C)

Checked with Cu2p3 spectra

Checked with C1s spectra

Since the presence of C-C is considered dominant, the energy gaps from C-C peak were used to the curve fitting.

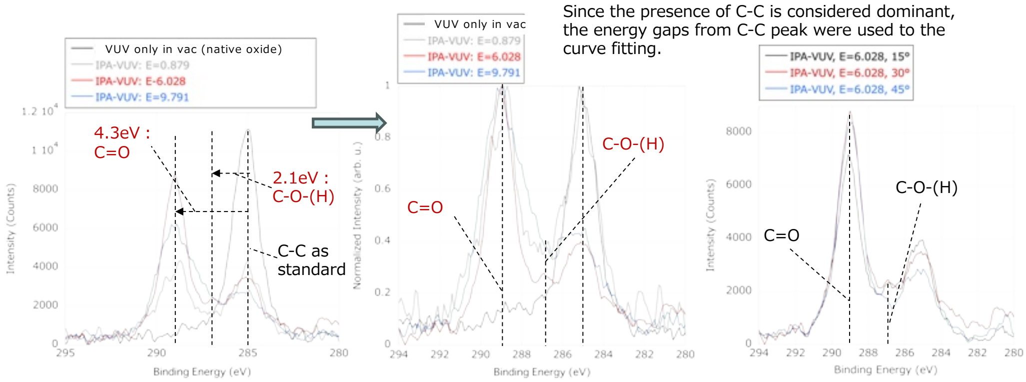

C1s spectra taken at 30° in different Exposure conditions

Normalized intensity to the maximum intensity in order to highlight the difference in binding conditions

Example of angle-resolved spectra at E=6.028. Taken at 15 and 30°.

35

3.2. Process Design

Evolution in bridge layer thickness according to Exposure :

- Layer growth has a saturation point : **About 2.4 s·kg/m³**
- Follows Freundlich's isotherm equation : Isotherm reaction between the solid-state surface and gas molecules occurring only at the surface of the bridge layer

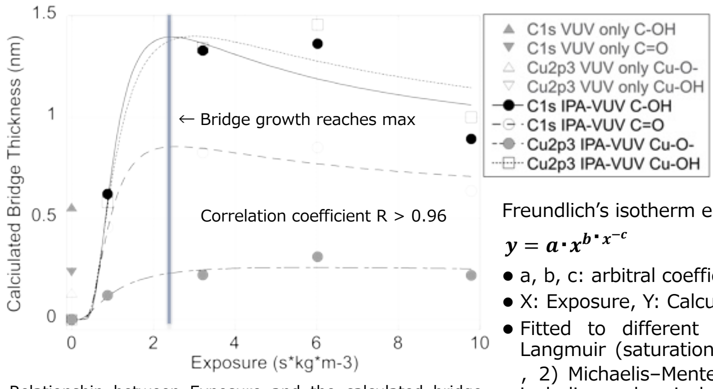

Relationship between Exposure and the calculated bridge layer thickness obtained from the curve fitting results of angle-resolved spectra.

- Approximate curve was forced to go 0 when E is 0, assuming that no beidge formation at E=0.
- Maximum point was evaluated from different element peaks.

Freundlich's isotherm equation :

$$y = a \cdot x^{b \cdot x^{-c}}$$

- a, b, c: arbitral coefficient
- X: Exposure, Y: Calculated bridge thickness
- Fitted to different isotherm equations . 1) Langmuir (saturation at monolayer formation) , 2) Michaelis–Menten equation (layer growth including chemical reaction inside) , 3) **Freundlich equation (successive adsorption, only at the top of the layer)**

3.2. Process Design

Bridge structure on Cu surface :

- Cu carboxylate at the bottom : **Bidentate coordination**
- Maximum thickness : **Arounf 2.5nm** (may be a little thicker in normal air)

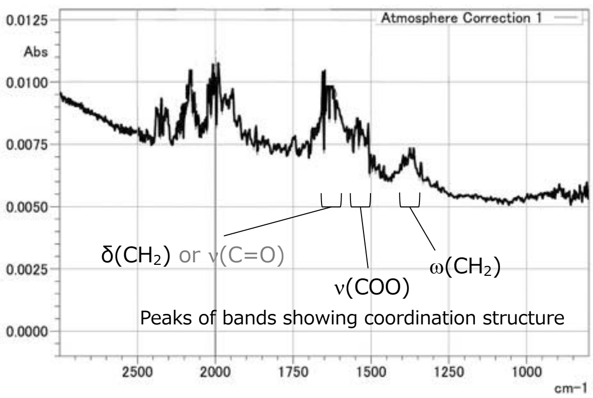

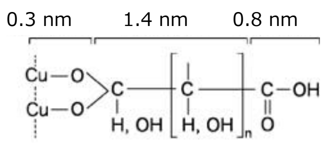

Schematic structure of Cu carboxylate derived from the results of XPS angle-resolved measurement and ATR-FTIR observation.

ATR-FTIR spectra of oxygen-free copper surface treated with IPA-VUV E=6.028 s·kg/m -3. Since the measurements were performed in air, the sample surface was exposed to air after the IPA-VUV treatment. Although the spectrum is noisy due to the small thickness of the bridge layer, a group of peaks of bands originating from the bidentate structure were observed. Ref : Fausto et al., J. Molecular Structure 349 (1995) 439.

3.3. Bondability & Debondability

- Shear strength of oxygen-free copper specimens bonded at Exposure near 2.4 s kg/m^{-3} : **>20 MPa, cohesive fracture**
- Since the overall shear strength is obtained by dividing the shear strength by the nominal bonded area, the true shear strength can be larger
- **No strength degradation** after 85%RH･85℃ storage testing for 1000 hours

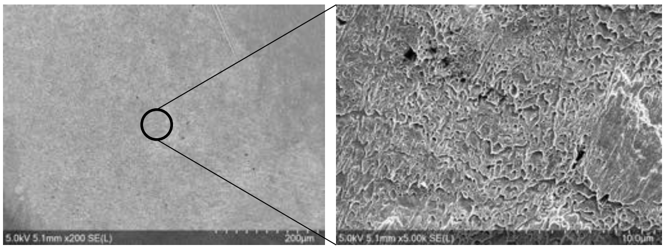

Scanning electron microscope (SEM) images of fracture surfaces after shear test of oxygen-free copper bonded under conditions near the maximum bridge formation condition. (Left) low magnification, (Right) high magnification. In the high-magnification image, cohesive fracture between surfaces is observed.

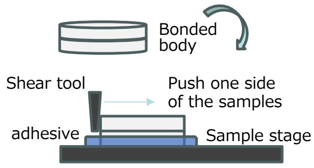

Schematic diagram of the shear test apparatus used in this study. The maximum shear load was 500 N. If the bond strength at the interface was larger and did not fracture, the load was applied repeatedly.

3.3. Bondability & Debondability

- Test sample: Kept at -60℃ for 24 hours (before the trigger temp)
- Transmission electron microscopy (TEM) observation: The bonded samples are thinned using a focused ion beam (FIB). The final thickness is about 80 nm, and the sample is exposed to air for about 72 hours before observation.
- There are some areas that appear to be contact defects caused by surface unevenness, but these areas are not cavities and are filled with bridge component.

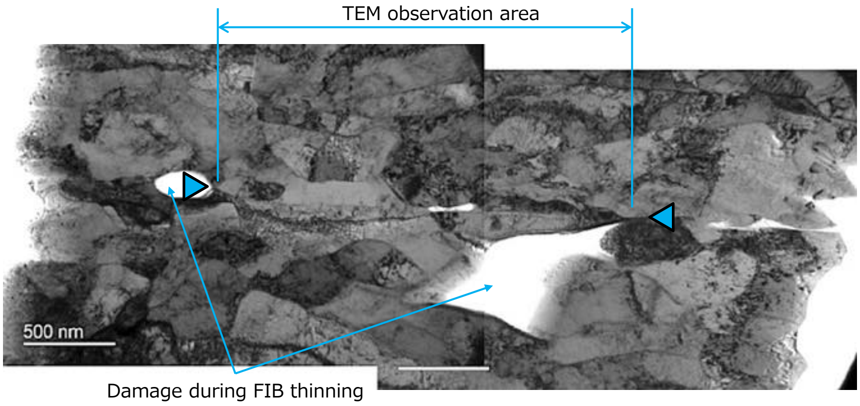

TEM low magnification image of the bond interface between oxygen-free Cu plates.

3.3. Bondability & Debondability

Nucleation of CuO nanoparticles was confirmed

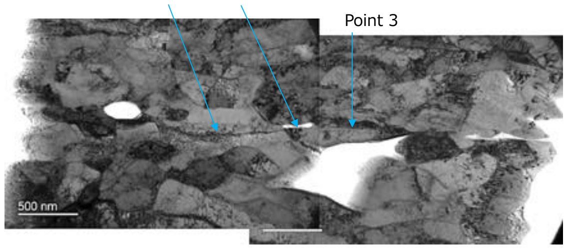

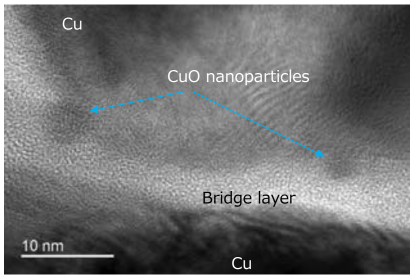

Point 3

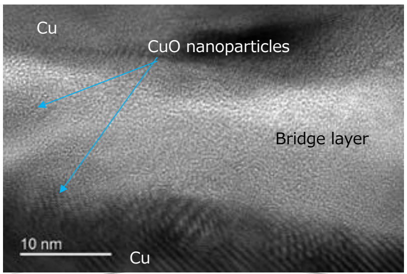

Point 1

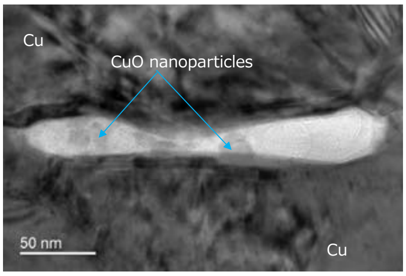

Point 2

TEM mid-magnification images

3.3. Bondability & Debondability

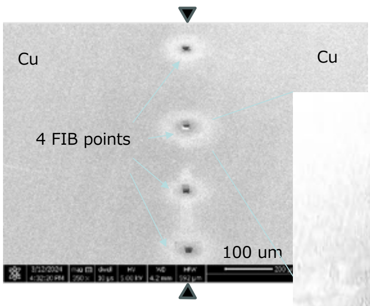

- **Kept at -95℃** for 24 hours (the trigger temp)
- FIB observation at 4 different positions on the interface

Uniform debonding was found in all FIB positions

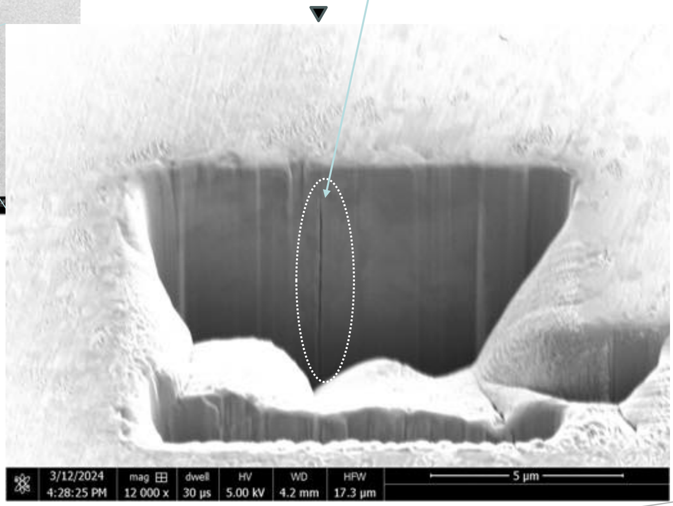

Summary

Muti-functional interfaces will be a key to next generation’s device integration. To achieve it via industrially simple way, V-VUV method is developed:

1. Seamless interconnection btwn BEOL & Adv. Pckg. is necessary
2. Low process temperature & non-vacuum is important
3. E-, IPA – VUV methods realized waterproof bondability
4. Debonding of Cu-Cu interface was feasible at around -100C
5. **Calculation for structural change is highly necessary now**

Thank you for your attention!

The research works in this presentation was/is supported by 1) Innovative Science and Technology Initiative for Security, 2) Scientific Research funding, and 3) LSTC. We thank for those successive supports.